

## Mode identification from line-profile variations

C. Aerts<sup>1</sup> & L. Eyer

*Instituut voor Sterrenkunde, Katholieke Universiteit Leuven, Belgium*  
*conny@ster.kuleuven.ac.be; laurent@ster.kuleuven.ac.be*

**Abstract.** We review the current status of different mode-identification techniques based on observed line-profile variations. Three basic methods are currently available to identify the non-radial pulsation modes. These three methods are described, together with their different variants. We further present applications to real data, focusing especially on  $\delta$  Scuti stars. After having discussed all the methods and their applications, we present an inventory in which we compare the properties of the different methods. Finally, we end with future prospects, both on the theoretical and observational side.

### 1. Introduction

Intrinsic variable stars are an important diagnostic to test stellar models, which provide in turn valuable clues to our understanding of stellar and galactic evolution. Variable stars pulsate in so-called *non-radial pulsation modes*. Since the early seventies, ample observational evidence of the presence of such non-radial pulsations has become available. From then on, detailed observational and theoretical studies of non-radial pulsations have been conducted. It has become clear that by understanding the pulsations in full detail, one can probe the internal structure of the stars and hence confront the results with stellar evolution theories, i.e., one can apply *asteroseismology*.

The non-radial pulsations lead to periodic variations of physical quantities, such as surface brightness, radial velocity, temperature, etc. By comparing the observed variations with those predicted by theory, it is in principle possible to determine the most important parameters that characterise the pulsation. One specific aspect of studying pulsations therefore is to know what kind of modes are active in pulsating variables, i.e., the aspect of *mode identification*. Specifically, mode-identification techniques try to assign values to the spherical wavenumbers  $(\ell, m)$ : the degree and azimuthal number of the spherical harmonic  $Y_\ell^m$  that describes the non-radial pulsation. The identification of non-radial pulsation modes from observational data of variable stars is important, since it is a first step towards asteroseismology. Indeed, the amount of astrophysical information that can be derived from the study of non-radial pulsations depends directly on the number of modes that can be successfully identified.

---

<sup>1</sup>Postdoctoral Fellow, Fund for Scientific Research, Flanders

Inspired by this potential of identifying the non-radial pulsation modes, the study of *mode-identification techniques* has become an extended topic by itself in variable star research. We have been involved in the development and the application of such mode-identification methods. In this review, we focus on the different identification techniques that are currently used to identify non-radial pulsations from line-profile variations.

The introduction of high-resolution spectrographs with sensitive detectors has had an enormous impact on the field of mode identification. Spectroscopic data usually offer a very detailed picture of the pulsation velocity field. On the other hand, they require large telescopes and sophisticated instrumentation. Before accurate detectors were available, identifications had to be obtained from photometric observations. These kind of data are suitable to study long-period pulsations because they can be obtained with small telescopes, which are available on longer time scales. For a review on photometric studies of  $\delta$  Scuti stars we refer to Poretti and to Garrido (these proceedings).

The plan of our paper is as follows. We first briefly give a (non-mathematical) introduction into the domain of non-radial pulsations. Next, we explain how a theoretical line profile can be calculated for a non-radially pulsating star. The following section is devoted to the description of the different identification techniques: line-profile fitting, Doppler Imaging, and the moment method. We briefly review the main characteristics of each method in Section 5 and we finally end with some future prospects in this field of research. In particular, we point out the importance of the identification of pulsation modes in  $\gamma$  Dor stars.

## 2. Non-radial pulsations

With a radial pulsation the physical parameters throughout a star vary periodically along the radial direction and spherical symmetry is preserved during a pulsation cycle. The differential equation describing the radial displacement is of the Sturm-Liouville type and thus allows eigensolutions that correspond to an infinitely countable amount of eigenfrequencies. The smallest frequency corresponds to the fundamental radial pulsation mode. The period of this mode is inversely proportional to the square root of the mean density of the star. Radial pulsations are characterised by the radial wavenumber  $n$ : the number of nodes of the eigenfunction between the center and the surface of the star.

If transverse motions occur in addition to radial motions, one uses the term non-radial pulsations. The pulsation modes are then not only characterised by a radial wavenumber  $n$ , but also by non-radial wavenumbers  $\ell$  and  $m$ . The latter numbers correspond to the degree and the azimuthal number of the spherical harmonic  $Y_\ell^m$  that represents the dependence of the mode on the angular variables  $\theta$  and  $\varphi$  for a star with a spherically symmetric equilibrium configuration (see Equation (1) below). The degree  $\ell$  represents the number of nodal lines, while the azimuthal number  $m$  denotes the number of such lines that pass through the rotation axis of the star. For stars that are not spherically symmetric, the expansion of the eigenfunctions in terms of spherical harmonics is no longer obvious.

A distinction is made between  $p$ -modes,  $g$ -modes, and  $r$ -modes. In  $p$ -modes, the restoring force is the pressure force; radial modes can be viewed as a special

case of non-radial  $p$ -modes. In  $g$ -modes, the restoring force is the buoyancy force; such modes have periods that are longer than the period of the radial fundamental mode. Finally,  $r$ -modes or toroidal modes are characterised by purely transverse motions; such modes only attain finite periods in rotating stars.

In the case of spheroidal modes in the approximation of a non-rotating star, the pulsation velocity expressed in a system of spherical coordinates  $(r, \theta, \varphi)$  centered at the centre of the star and with polar axis along the symmetry axis of pulsation, is given by

$$\vec{v}_{\text{puls}} = (v_r, v_\theta, v_\varphi) = N_\ell^m v_p \left( 1, K \frac{\partial}{\partial \theta}, \frac{K}{\sin \theta} \frac{\partial}{\partial \varphi} \right) Y_\ell^m(\theta, \varphi) \exp(i\omega t) \quad (1)$$

(e.g., see Smeyers 1984, Unno et al. 1989). In this expression,  $N_\ell^m$  is the normalisation factor for the  $Y_\ell^m(\theta, \varphi)$  over the visible hemisphere of the star,  $v_p$  is the pulsation amplitude,  $\omega$  is the pulsation frequency, and  $K$  is the ratio of the horizontal to the vertical velocity amplitude. The latter can be found from the boundary conditions:  $K = GM/(\omega^2 R^3)$ . The sign of the azimuthal number  $m$  describes how the mode progresses with respect to the rotation of the star. We here adopt the convention that positive  $m$ -values represent waves that travel opposite to the rotation (retrograde modes), while negative  $m$ -values are associated with modes that travel in the direction of the rotation (prograde modes). Modes with  $m = 0$  are axisymmetric modes, while those with  $\ell = |m|$  are called sectoral modes. In all other cases ( $\ell \neq |m|$  and  $m \neq 0$ ) one speaks of tesseral modes.

A caveat for many analyses on non-radial pulsations is that the theoretical framework that is used only applies in the slow-rotation approximation, i.e., in the case where the effects of the Coriolis force and of the centrifugal forces can be neglected in deriving an expression for the components of the pulsation velocity. We emphasize that it is not allowed to describe an oscillation mode for a rotating star in terms of a single spherical harmonic, and so to ascribe a single set of wavenumbers  $(\ell, m)$  to a mode. The Coriolis force, for instance, introduces a transverse velocity field that is of the same order of magnitude as the pulsation velocity for a non-rotating star if the ratio  $\Omega/\omega$  of the rotation frequency to the pulsation frequency approaches unity. In particular, we have studied the effect of the Coriolis force on line-profile variations in the case of  $p$ -modes (Aerts & Waelkens 1993) and we have found that the line profiles can be largely influenced for some stellar parameters. A comparable study for  $g$ -modes was presented by Lee & Saio (1990). For stars having  $\Omega/\omega \approx 1$  or larger, the centrifugal forces also become important. Including the latter enormously increases the complexity of the mathematical treatment of the problem, because deviations from spherical symmetry have to be taken into account. It is clear that  $\Omega/\omega$ -values, which are too large to be neglected if the aim is to obtain an accurate description of the pulsation, are met in several stars discussed in the literature. A re-evaluation of observed line profiles in rapid rotators is therefore necessary in some cases.

### 3. Line-profile variations

The velocity field caused by the non-radial pulsation(s) leads, through Doppler displacement, to periodic variations in the profiles of spectral lines. Theoretical line-profile variations can be calculated in the following way. Consider a system of spherical coordinates  $(r, \theta, \varphi)$  with the polar axis coinciding with the direction to the observer. The velocity field due to the rotation and the pulsation leads to a Doppler shift at a point  $(R, \theta, \varphi)$  on the visible surface of the star. The local contribution of a point  $(R, \theta, \varphi)$  to the line profile is proportional to the projected intensity of that point. We approximate this projected intensity as follows. We divide the stellar surface into a number of infinitesimal surface elements, which, for computational purposes, have finite dimensions. Next, we assume that the intensity  $I_\lambda(\theta, \varphi)$  is the same for all points of the considered surface element. The projected intensity of the surface element surrounding the point  $(R, \theta, \varphi)$  then is the product of the intensity  $I_\lambda(\theta, \varphi)$  and the projection on the line of sight of the surface element around the considered point:

$$I_\lambda(\theta, \varphi) R^2 \sin \theta \cos \theta \, d\theta \, d\varphi. \quad (2)$$

Because of variations of the intensity over the stellar surface, and of the temperature dependence of an absorption line, the contributions of the different points on the visible stellar surface to the line profile have a different amplitude. In first instance, however, one assumes that the perturbations of the intensity and of the surface affect the line profile only slightly. These effects are therefore neglected and it is assumed that  $\delta I_\lambda(\theta, \varphi) = 0$  during the pulsation. The time dependence of the intensity is important when the spectral line is sensitive to the temperature and when the temperature differs for different points on the stellar surface. This time dependence is also neglected in most calculations.

The most important effect that then changes the projected intensity over the visible surface is the limb darkening. Usually, the intensity is assumed to be isotropic in the  $\varphi$  coordinate and the  $\theta$ -dependence of the intensity is described by a limb-darkening law of the form

$$h_\lambda(\theta) = 1 - u_\lambda + u_\lambda \cos \theta, \quad (3)$$

where  $u_\lambda \in [0, 1]$  is called the limb-darkening coefficient; it depends on the considered wavelength range. Wade & Rucinski (1985) have tabulated limb-darkening coefficients in terms of temperature, gravity and wavelength. The projected intensity of a surface element centered around the point  $P(R, \theta, \varphi)$  with size  $R^2 \sin \theta \, d\theta \, d\varphi$  then is

$$I_0 h_\lambda(\theta) R^2 \sin \theta \cos \theta \, d\theta \, d\varphi, \quad (4)$$

where  $I_0$  is the intensity at  $\theta = 0$ .

In order to take into account intrinsic broadening effects, the local line profile is convolved with an intrinsic profile, which we take to be Gaussian with variance  $\sigma^2$ , where  $\sigma^2$  depends on the spectral line considered. Generalisations to an intrinsic Voigt profile or a profile derived from a stellar atmosphere model are easily performed.

Let us represent by  $p(\lambda)$  the line profile and by  $\lambda_{ij}$  the Doppler-corrected wavelength for a point on the star with coordinates  $(\theta_i, \varphi_j)$ , i.e.,

$$\frac{\lambda_{ij} - \lambda_0}{\lambda_0} = \frac{\lambda(\theta_i, \varphi_j) - \lambda_0}{\lambda_0} = \frac{\Delta\lambda(\theta_i, \varphi_j)}{\lambda_0} = \frac{v(\theta_i, \varphi_j)}{c} \quad (5)$$

with  $v(\theta_i, \varphi_j)$  the component of the sum of the pulsation and rotation velocity of the considered point in the line of sight. An explicit expression for  $v(\theta_i, \varphi_j)$  can be found in e.g., Aerts et al. (1992). The line profile can then be approximated as

$$p(\lambda) = \sum_{i,j} \frac{I_0 h_\lambda(\theta_i)}{\sqrt{2\pi}\sigma} \exp\left(-\frac{(\lambda_{ij} - \lambda)^2}{2\sigma^2}\right) R^2 \sin\theta_i \cos\theta_i \Delta\theta_i \Delta\varphi_j, \quad (6)$$

where the sum is taken over the visible stellar surface ( $\theta \in [0^\circ, 90^\circ]$ ,  $\varphi \in [0^\circ, 360^\circ]$ ).

We show in Figures 1 and 2 sets of theoretically calculated profiles for  $\ell = 2$  and  $\ell = 6$  modes. The profiles in Figure 1 are for prograde modes, those in Figure 2 for retrograde modes. The other velocity parameters are  $v_p = 5$  km/s,  $v \sin i = 30$  km/s,  $\sigma = 4$  km/s, and  $i = 55^\circ$ . Other studies in which theoretical profiles are given are published by Kambe & Osaki (1988) and by Schrijvers et al. (1997).

Ideally, the calculation for the line profile described above should be generalised in order to take into account the following additional time-dependent effects: a variable surface normal, a variable intensity through non-adiabatic temperature variations, a variable intrinsic profile, Coriolis and centrifugal correction terms to the pulsation velocity expression. The most up-to-date code that takes into account some of these effects is written by Townsend (1997). He used Lee et al. 's (1992) formalism to take into account rotation effects. This formalism incorporates the Coriolis force for all values of  $\Omega/\omega$ , but neglects the centrifugal forces, which are  $\sim \Omega^2$ . A variable surface normal is taken into account, but the intensity variations are still assumed to be adiabatic according to the approximation presented by Buta & Smith (1979). This user-friendly code published by Townsend (1997) is available upon request from the author.

#### 4. Identification techniques

In this section, we describe the different methods that are used to identify modes. It is clear that the velocity expression based on the non-radial pulsation model presented above contains many free parameters, even in the simple formulation in which rotational and non-adiabatic effects are neglected. Especially the infinity of candidate modes is a problem when constructing identification techniques and it often keeps the predictive power of the methods low. This is in particular the case for the methods that are based on a trial-and-error principle. We point out that quantitative methods are better to obtain a reliable mode identification. This need for quantitative methods has become apparent since more and more detailed spectroscopic analyses have revealed that multimode pulsations are often present. Below, we treat three methods, more or less in the order of their appearance in the literature.

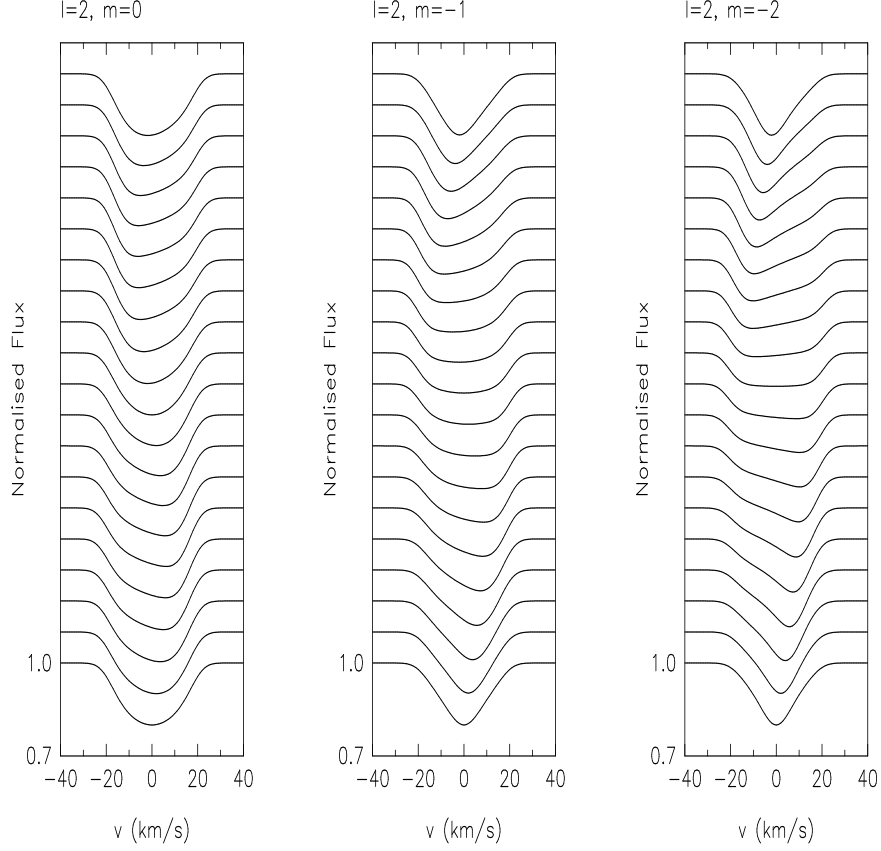


Figure 1. Theoretically determined line-profile variations calculated by means of the basic formalism given in Section 3. We used an  $\ell = 2$  mode and respectively  $m = 0$  (left panel),  $m = -1$  (middle panel), and  $m = -2$  (right panel). The other velocity parameters are:  $v_p = 5$  km/s,  $v \sin i = 30$  km/s,  $\sigma = 4$  km/s, and  $i = 55^\circ$ . The phase of each profile increases from 0.0 (lowest profile) to 1.0 (highest profile) in steps of 0.05.

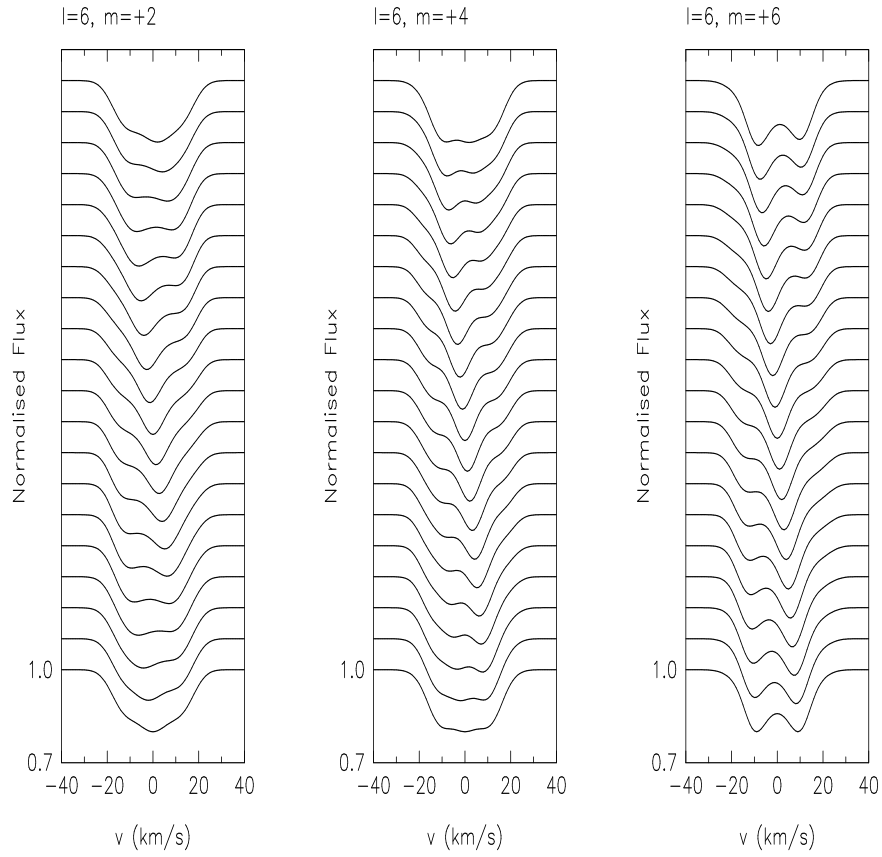


Figure 2. The same as in Figure 1, but for  $\ell = 6$  with  $m = +2$  (left panel),  $m = +4$  (middle panel), and  $m = +6$  (right panel).

In describing the methods, we assume that the pulsation frequencies have been determined from the observables of the variable stars. For a description of the different methods used to derive the modal frequencies, we refer to the review of Mantegazza: Mode detection from line-profile variations (these proceedings). We pay special attention to describe applications to  $\delta$  Scuti stars in this paper. For a review on identification methods applied to OB-type variables we refer to Aerts (1994).

#### 4.1. Objective line-profile fitting

Since Osaki (1971) computed theoretical line profiles for various non-radial pulsations, the identification of modes from spectroscopic observations has become possible. The identification of non-radial pulsation modes from line-profile variations was first achieved by line-profile fitting on a trial-and-error basis. The idea is to compare the observed line-profile variations with those predicted by theoretical calculations. This technique was the first one in use to identify modes from spectroscopic observations.

Pioneering work in the field of line-profile fitting was done by M. Smith and his collaborators. They obtained line profiles for various types of pulsating stars. We show in Figure 3 their observed line profiles, represented as dots, of the  $\delta$  Scuti star  $\rho$  Puppis (Campos & Smith 1980b). The theoretical profiles that are presented by the full line are constructed with a radial mode. The dashed curves represent rotationally broadened lines, i.e., lines for a non-pulsating star. These dashed lines show that the line profiles of  $\rho$  Puppis are indeed variable in time because of the pulsation of the star. The representation by the full line is rather faithful and the authors concluded that the star pulsates radially. Later on, it was found by means of the moment method applied to more recent spectra (see Figure 4 and Section 4.3) that the main mode is indeed radial, but that at least one, and probably two, additional small-amplitude modes are present in  $\rho$  Puppis (Mathias et al. 1997), a conclusion that would have been very hard to obtain by means of the fitting technique.

In the seventies and early eighties, the fitting technique by trial-and-error was very popular, simply because it was the only one available. Besides applications in the case of  $\delta$  Scuti stars (Campos & Smith 1980b, Smith 1982), the technique was also applied to line-profile variations of  $\beta$  Cephei stars (Smith 1977, 1983; Campos & Smith 1980a), Be stars (e.g., Vogt & Penrod 1983, Baade 1984), and the so-called 53 Per stars (Smith 1977, Smith et al. 1984). Smith (1982) describes mode-typing for 9  $\delta$  Scuti stars by means of line-profile fitting. Most of the results that he obtained are still valid today as far as the main modes of the stars are concerned.

As already mentioned, the main disadvantage of the trial-and-error line-profile fitting is the large number of free parameters that appear in the velocity expression due to the non-radial pulsation. In principle, the complete free parameter space has to be scanned before a decision on the best mode can be obtained. This was not yet possible some 15 years ago, because it was computationally too demanding. For this reason, only a limited number of combinations were tried out, with the result that the identification technique was not very objective. Moreover, the non-radial pulsation model can be quite successful in reproducing the line profiles observed on a short time scale for different sets



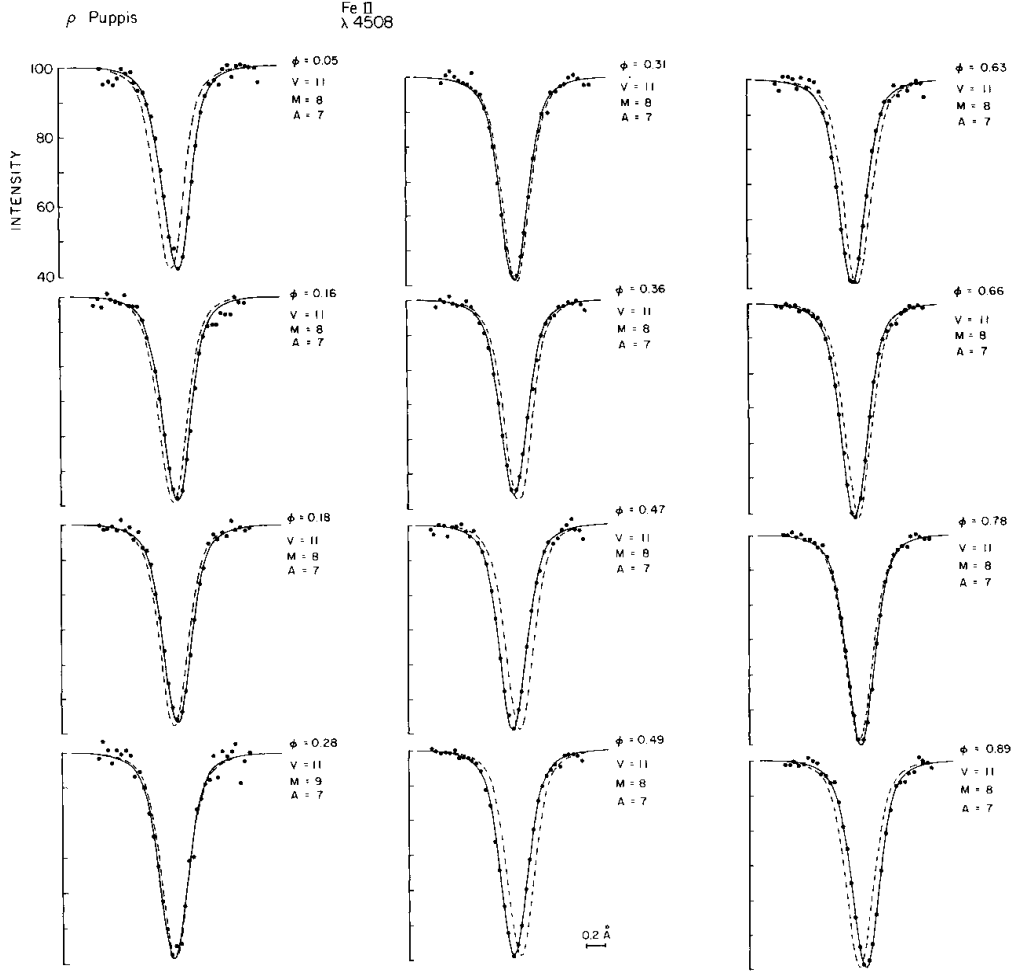


Figure 3. Observed (dots) and theoretical line-profile variations of the  $\delta$  Scuti star  $\rho$  Puppis. The full line is a model for a radial pulsation while the dashed line is a model for which only rotational broadening appears.  $V$  stands for the projected rotation velocity,  $M$  for the intrinsic broadening, and  $A$  for the amplitude of the pulsation; these three velocities are indicated next to each panel and are expressed in km/s. Figure taken with permission from Campos & Smith (1980b).

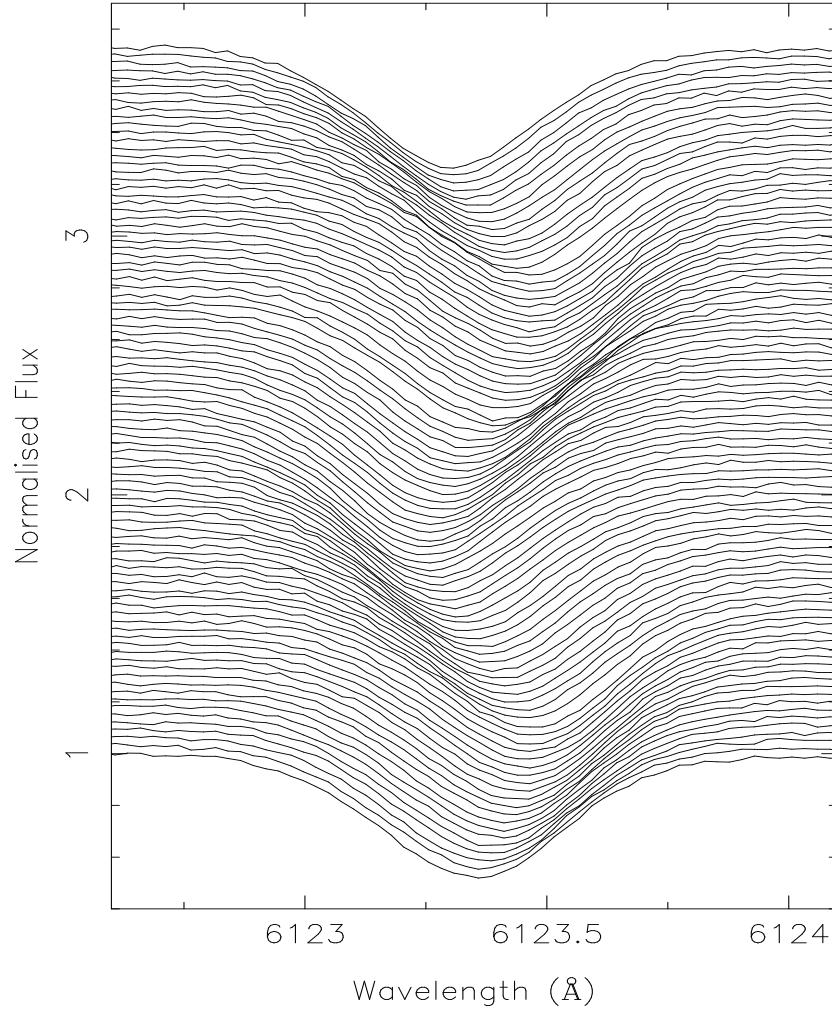


Figure 4. Line-profile variations of the  $\delta$  Scuti star  $\rho$  Puppis observed with the CAT/CES of ESO by Mathias et al. (1997). The quality of these data are much better than those presented in Figure 3. They have revealed the presence of additional small-amplitude modes, besides the main radial mode.

of input parameters, i.e., the fitting technique does not necessarily lead to a unique solution. We also point out (see Aerts et al. 1992, Aerts & Waelkens 1993) that the apparent quality of some fits is suspect in the sense that in early modeling, one neglected temperature variations and rotational effects, which obviously must affect the profiles in some cases (Lee et al. 1992).

Other problems that appeared in early applications of the line-profile-fitting technique are caused by the often very limited time base of the data, because of which it was sometimes necessary to assume that modes temporarily disappear in order to re-obtain good fits for new data that span a longer time scale. Also, the values found for the intrinsic profile sometimes had to be varied from one night to another in order to obtain reliable fits. In the case of rapidly rotating stars, one usually assumed equator-on geometries and high-degree sectoral modes because these are the ones that best reproduce the observed moving bump phenomenon. Finally, it was mentioned, but most often not taken into account for applications to rapid rotators, that one used an expression for the pulsation velocity that is related to one spherical harmonic. This is, however, only valid in the case of a non-rotating star. All the abovementioned assumptions were introduced in an *ad hoc* fashion and cast doubt on the reliability of the model.

Nowadays, it is possible to identify the pulsation mode by performing line-profile fitting in an objective way. This can be achieved by calculating a kind of overall standard deviation per wavelength pixel between theoretically determined and observed profiles for a large grid of possible wavenumbers and velocity parameters. In order to do so, one needs a large homogeneous data set of high-resolution profiles that are well-spread over the period that appears in the line-profile variability. The theoretical limitations of the model have also mostly been overcome by now, as explained in Section 3.

A plus point of objective line-profile fitting is that both the wavenumbers ( $\ell, m$ ) and all the other velocity parameters are derived. In this way, the complete motion due to pulsation can be reconstructed once the best fit is selected.

THE major drawback of objective line-profile fitting is that it is still limited to a monoprotic pulsation. Indeed, it is in practice impossible to consider combinations of all kinds of different modes to fit the data without any restriction on the parameters. It is nevertheless useful to use fitting for multiperiodic stars, once estimates of the spherical wavenumbers and the velocity parameters are at hand from other methods such as those presented in the following two sections.

## 4.2. Doppler Imaging

In recent spectroscopic studies, a lot of attention has been paid to the line-profile variations of rapidly rotating OB stars. This has been in particular the case since it was recognised that the line profiles of rapid rotators allow a Doppler Imaging of the stellar surface (Vogt et al. 1987), so that a mapping of the velocity over this surface is possible (Baade 1987).

Gies & Kullavanijaya (1988) first presented an objective criterion based on Doppler Imaging to determine the periods and pulsation parameters of the modes in the rapidly rotating line-profile variable B 0.7 III star  $\epsilon$  Per. In Figure 5 we show a grey-scale representation of the residual line-profile variations (with respect to the global symmetric line profile) of  $\epsilon$  Per obtained on 26 November 1996. Black denotes local deficiencies of the flux and white local increments.

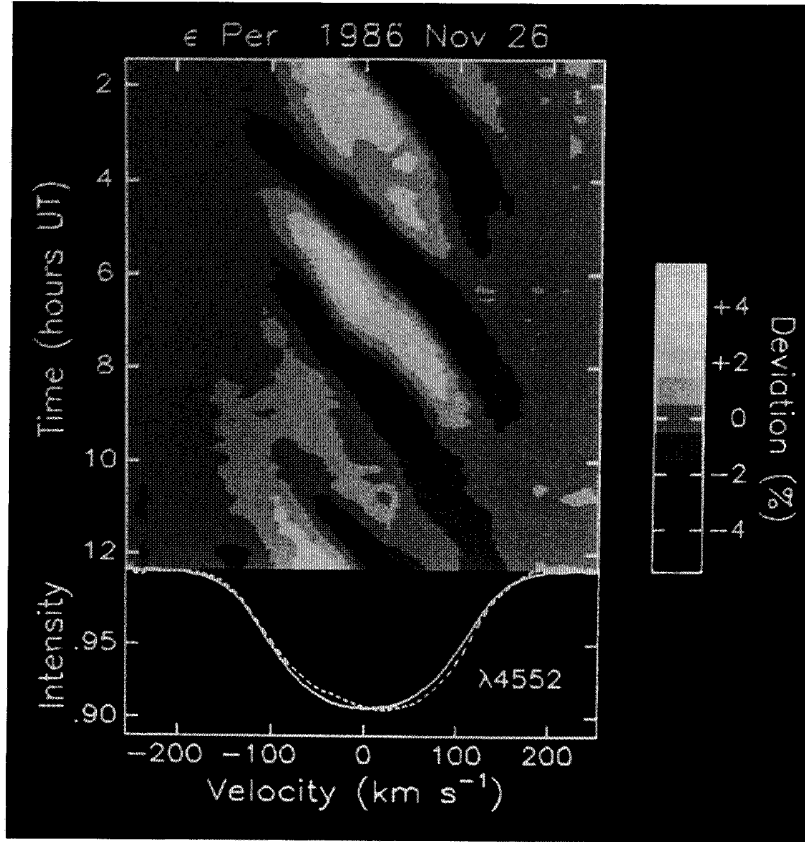


Figure 5. Grey-scale representation of the observed line-profile variations of  $\epsilon$  Per. The spectra are residuals with respect to the global average line profile, shown as full line in the lower panel. The dashed line is the nightly average profile. Darker shades indicate a depression relative to the mean line while bright regions correspond to places where the profile is shallower than the mean. Figure taken from Gies & Kullavanijaya (1988) with permission.

Gies & Kullavanijaya noted that emission patterns that move through the line profile during the pulsation cycle are easily detected and visualised in such a representation. This way of presenting data has since then become very popular. Fourier analysis of the line-profile variations at each wavelength point yields the periods of the variations by frequency peaks in the resulting periodogram.

Subsequently, the azimuthal number  $m$  is obtained by considering the number of phase changes  $\Delta(\text{Phase})$  at each signal frequency versus the line position. These observed phase changes are shown in Figure 6 in the case of the four frequencies detected by Gies & Kullavanijaya in their line-profile variations of  $\varepsilon$  Per. The basic idea behind the estimation of  $m$  is the following. Let us **assume** that sectoral modes are excited, that we are dealing with an equator-on view and that the bump motion is caused by the large rotation of the star. Since each of the three components of  $\vec{v}_{\text{puls}}$  is proportional to  $\exp(i(\omega t + m\varphi))$ , the phase decreases by  $m/2$  cycles between the blue and the red wing of the profile. In this way, an upper limit of  $m$  is given by  $2\Delta(\text{Phase})$ . On the other hand,

$$\frac{d\text{Phase}/d\varphi}{dV_{\text{rot}}/d\varphi} = \frac{m/2\pi}{V_{\text{eq}} \sin i \sin \theta \cos \varphi}, \quad (7)$$

where  $V_{\text{rot}}$  is the component of the rotation velocity in the line-of-sight and  $V_{\text{eq}}$  stands for the equatorial rotation speed. In this way,

$$2\pi(V_{\text{eq}} \sin i) \frac{d(\text{Phase})}{dV_{\text{rot}}} \quad (8)$$

is a lower limit for  $m$ . By calculating both limits, one obtains an estimate of the azimuthal number of the mode.

Table 1. The limits for the azimuthal number  $m$  for the star  $\varepsilon$  Per as derived by Gies & Kullavanijaya (1988)

Signal	Lower Limit	Upper limit	Adopted
S3	-3.93	-2.98	-3
S4	-4.42	-3.60	-4
S5	-5.15	-4.46	-5
S6	-6.90	-5.20	-6

In Table 1 we list the limiting values for the azimuthal number  $m$  obtained by Gies & Kullavanijaya (1988) from the observed phase changes shown in Figure 6. Additional frequencies and interpretations of the line-profile variability of  $\varepsilon$  Per are available by now (see e.g., Gies et al. 1999), but we do not want to describe the details here since the  $\varepsilon$  Per case was only given as an example of the method.

A major disadvantage of the Doppler Imaging method as proposed by Gies & Kullavanijaya (1988) is that equator-on-viewed sectoral modes are assumed without a real physical argument. For this and also other reasons, a number of generalisations of the method have been proposed in the literature. Merryfield & Kennelly (1993) propose to use the Doppler Imaging principle to obtain the

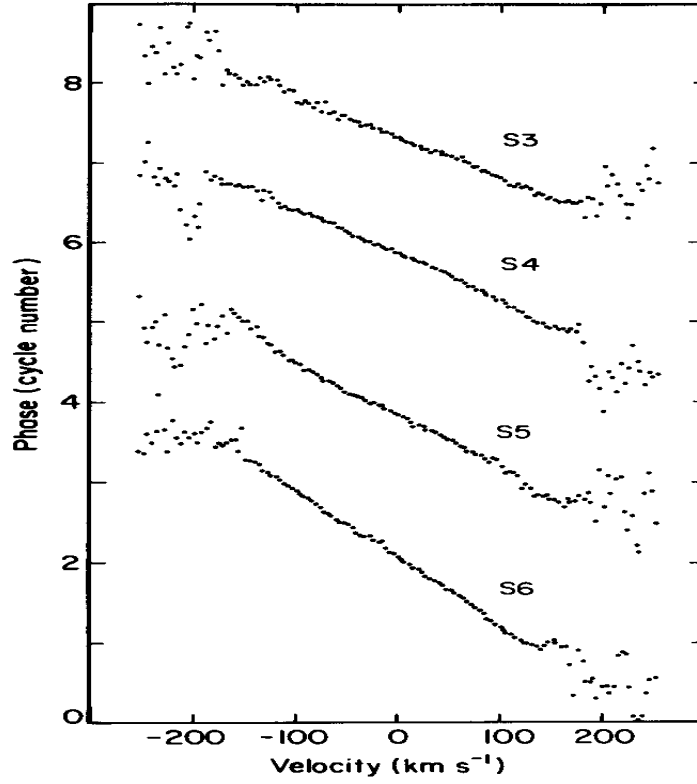


Figure 6. The phase of the power spectrum of the line-profile variations of  $\epsilon$  Per as a function across the line profile. Each plot corresponds to the phases at the peak frequencies S3, S4, S5, S6 that were found in the profile variations. An estimate of the azimuthal number  $m$  is derived from these phase changes (see text for an explanation). Figure taken from Gies & Kullavanijaya (1988) with permission.

wavenumbers by considering a two-dimensional Fourier transform, which leads to power diagrams as a function of the frequency and as a function of what they call the “apparent” azimuthal number  $\hat{m}$ . They propose that  $\hat{m}$  may be an estimate of the degree rather than the azimuthal number in the case of tesseral modes. This finding was unambiguously proven for the first time for all considered modes by Telting & Schrijvers (1997), who performed an extensive simulation study to evaluate the Doppler Imaging method as an identification method. They also found that the phase variation for the first harmonic of the frequency contains information on the azimuthal number  $m$ . So far, Schrijvers & Telting applied their method to (new)  $\beta$  Cep stars (for an overview of their applications, see Schrijvers 1999).

Kennelly & collaborators (Kennelly et al. 1992a:  $\tau$  Peg; 1992b:  $\gamma$  Boo; 1996:  $\theta^2$  Tau; 1998a:  $\varepsilon$  Cep) are the only ones so far who have actually used the Doppler Imaging principle to obtain the wavenumbers for a group of rapidly rotating  $\delta$  Scuti stars. Hereto, they gathered numerous high-quality spectra and they considered a two-dimensional Fourier transform. Their latest technique consists of the following two steps:

- perform a DDLPV: Doppler Deconvolution of line-profile variations. First, one derives the intrinsic profile  $\psi(v)$  from the deconvolution  $\bar{\phi}(v) = R(v) * \psi(v)$ , where  $\bar{\phi}(v)$  is the time-averaged line profile and  $R(v)$  the rotationally broadened profile. As first guess for  $\psi$ , the synthetic spectrum from a model atmosphere is taken. Subsequently, the observed time-dependent pulsationally broadened components  $\phi(v, t)$  of the spectra are modeled from the deconvolution  $\phi(v, t) = B(v, t) * \psi(v)$ . As initial guess for  $\phi$  they take the rotational broadening  $R$ .

In Figure 7 we show the result of the DDLPV technique applied by Kennelly et al. (1998a) to their line-profile variations of the  $\delta$  Scuti star  $\varepsilon$  Cep.

- perform FDI: Fourier Doppler Imaging, by remapping the time-variable component of  $B(v, t)$  from velocity to Doppler space  $B(\phi, t)$  by means of  $\phi_i = \sin^{-1}(v_i/v \sin i)$ . Next, the two-dimensional Fourier transform of  $B(\phi, t)$ , and the corresponding amplitude spectrum, is computed.

We refer to Kennelly et al. (1998b) for more details, but we point out here that  $\bar{\phi}(v)$  also contains a broadening component due to the pulsation which is not taken into account by the authors.

The only assumption that Kennelly et al. (1998a) use is that the rotation causes the bump motion (i.e.,  $v \ll v \sin i$ ) and that an accurate estimate of the rotational velocity is known. We show in Figure 8 the two-dimensional amplitude spectrum of  $\varepsilon$  Cep, obtained from Fourier Doppler Imaging of the time-variable component of the broadening function in Doppler space and time. The measured frequencies are indicated as crosses (Kennelly et al. 1998a).

The Doppler Imaging technique is not really suited to analyse data sets that contain very few spectra per night. In this sense, its applicability is limited to short-period pulsators (i.e.,  $p$ -mode pulsators) for which one usually focuses on one or a few stars per night during an observing mission with a time base of typically a week. The observing strategy with long-term spectroscopy, which is necessary to analyse the line-profile variations of  $g$ -mode pulsators, is totally

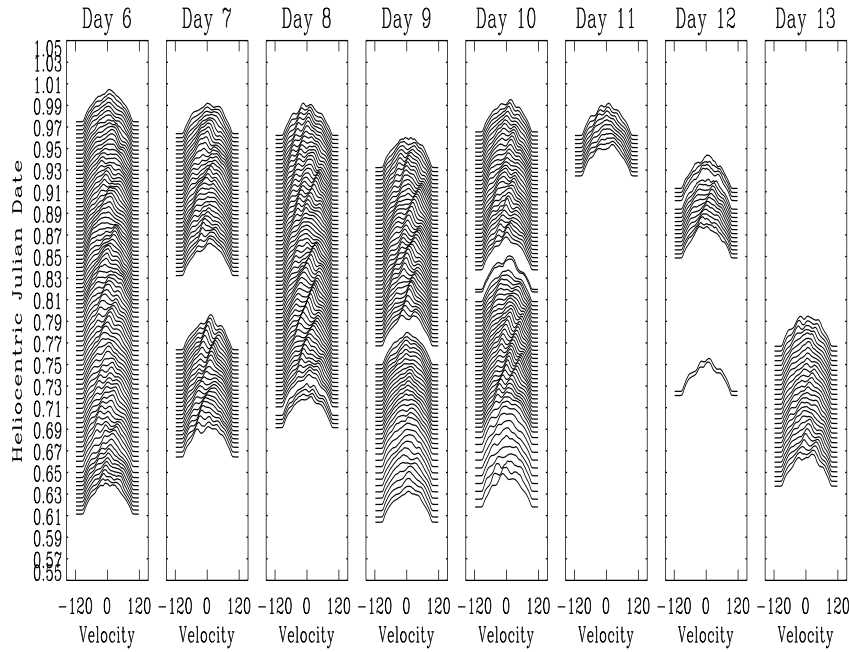


Figure 7. Time series of broadening functions of  $\varepsilon$  Cep using the DDLPV technique (see text for an explanation). The profiles are plotted as a function of Doppler shift and time. Patterns of variation owing to the pulsations of the star can be seen as bumps which travel through the profiles. Figure taken from Kennelly et al. (1998a) with permission.

different. In this case one takes a large sample of stars which are each measured between two and five times per night during weeks that are in their turn separated by months (for an example of a long-term spectroscopic project, see Aerts et al. 1999a). Grey-scale representations and identification methods as the ones shown in Figure 5 and Figure 6 become meaningless in this case, the more so because most  $g$ -mode pulsators found up to now are slow rotators.

THE major problem with the Doppler Imaging technique, in whatever form, is that the spherical wavenumbers are estimated from diagnostics that are not immediately interpretable in terms of the physics involved in the pulsational displacement. Indeed, the underlying mathematical basis for this method is lacking. A first effort to link the physical quantities directly to the amplitude and phase in Fourier space was undertaken by Hao (1998). This effort did not lead to new results compared with those already obtained by Telting & Schrijvers (1997) from their simulation study and does not give any information on the velocity parameters other than the degree of the pulsation. In fact, only one, and in the best case the two, wavenumber(s) is (are) estimated as real number(s) from the observed phase changes. A real value of  $\ell$  and  $m$  has, however, no physical meaning. Moreover, no information can be derived, for example, for the amplitude of the pulsation and for the inclination angle. On the other hand,



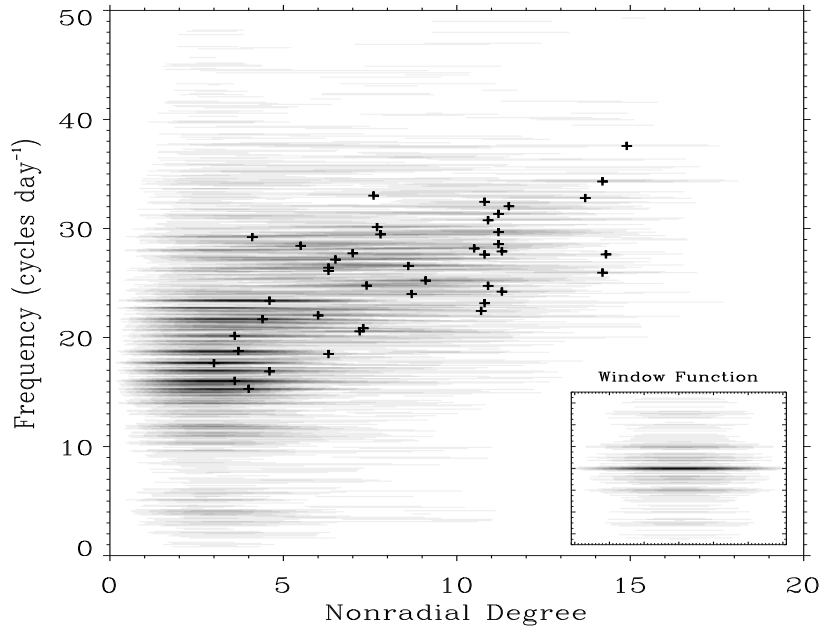


Figure 8. The two-dimensional Fourier amplitude spectrum and frequency analysis of  $\varepsilon$  Cep. The spectrum was computed using the Fourier Doppler Imaging technique (see text for an explanation). The window function for the spectrum is illustrated as an inset. The frequencies identified by the two-dimensional frequency analysis are indicated as crosses. Figure taken from Kennelly et al. (1998a) with permission.

multiperiodicity is easily taken into account, contrary to the other methods. We therefore advise to combine Doppler Imaging with line-profile fitting once the best estimates of  $(\ell, m)$  for each of the modes are obtained. We finally recall that the method is only applicable to rapid rotators because of the basic assumption that the rotation carries bumps across the profiles. For the same reason it is also unsuitable to detect axisymmetric modes ( $m = 0$ ) and low-degree tesseral modes.

#### 4.3. The moment method

As an alternative to the line-profile-fitting technique, Balona (1986a, b; 1987; 1990) proposed a new method to identify the modes from line-profile variations: *the moment method*. This method is based on the time variations of the first few moments of a line profile. We have extended this method and applied it for the first time to line-profile variations of a real star, namely the monoprotodic  $\beta$  Cephei star  $\delta$  Ceti (Aerts et al. 1992). In the meantime, this method turned out to be the best identification technique for slow rotators. We here briefly sketch the basic ideas of the moment method in our formulation (see Aerts 1996 for the latest version).

Since a line profile is a convolution (see Equation (6)) of an intrinsic profile (here denoted by  $g(v)$ ) and the intensity in the direction of the observer integrated over the visible surface (denoted by  $f(v)$ ), the  $n$ th moment of a line profile  $(f * g)(v)$  is defined as

$$\langle v^n \rangle_{f*g} \equiv \frac{\int_{-\infty}^{+\infty} v^n f(v) * g(v) dv}{\int_{-\infty}^{+\infty} f(v) * g(v) dv}, \quad (9)$$

where  $v$  is the total velocity component in the line of sight. In principle, all the moments are needed to give a complete description of the line profile, but we have shown that the first three moments contain enough information to accurately describe the profiles (Aerts et al. 1992, De Pauw et al. 1993). Note that normalised moments are considered such that they are only slightly influenced by temperature variations and by uncertainties in the intrinsic profile.

We have shown that, in the slow-rotation approximation, the first three moments of a monoprotodic pulsation with frequency  $\omega$  are given by :

$$\langle v \rangle_{f*g} = v_p A(\ell, m, i) \sin[(\omega - m\Omega)t + \psi], \quad (10)$$

$$\begin{aligned} \langle v^2 \rangle_{f*g} = & v_p^2 C(\ell, m, i) \sin[2(\omega - m\Omega)t + 2\psi + \frac{3\pi}{2}] \\ & + v_p v_\Omega D(\ell, m, i) \sin[(\omega - m\Omega)t + \psi + \frac{3\pi}{2}] \\ & + v_p^2 E(\ell, m, i) + \sigma^2 + b_2 v_\Omega^2, \end{aligned} \quad (11)$$

$$\begin{aligned}
\langle v^3 \rangle_{f*g} = & v_p^3 F(\ell, m, i) \sin[3(\omega - m\Omega)t + 3\psi] \\
& + v_p^2 v_\Omega G(\ell, m, i) \sin[2(\omega - m\Omega)t + 2\psi + \frac{3\pi}{2}] \\
& + \left[ v_p^3 R(\ell, m, i) + v_p v_\Omega^2 S(\ell, m, i) + v_p \sigma^2 T(\ell, m, i) \right] \\
& \times \sin[(\omega - m\Omega)t + \psi]
\end{aligned} \tag{12}$$

(Aerts et al. 1992). In these expressions,  $\psi$  is a phase constant depending on the reference epoch,  $i$  is the inclination angle between the rotation axis and the line of sight,  $v_\Omega$  is the projected rotation velocity (a uniform rotation is assumed),  $b_2$  is a constant depending on the limb-darkening function,  $\sigma$  again represents the width of the Gaussian intrinsic profile as in Section 3, and the functions  $A, C, D, E, F, G, R, S, T$  depend on the kind of mode and on the inclination. They contain the complete physics of the pulsation. For an explicit expression of these functions, we refer to Aerts et al. (1992), but we point out here that these functions are the same for positive and negative azimuthal numbers because the slow-rotation approximation is used. It is then impossible in this description to decide from the moments how a mode travels with respect to the rotation.

By means of an example, we show in Figure 9 the first three moments of the Ca I  $\lambda\lambda 6122.21\text{\AA}$  line observed for the  $\delta$  Scuti star  $\rho$  Puppis. The observed moments are fitted with a monoprotic pulsation model for the frequency  $f = 7.098168 \text{ c/d}$  (for a full description of the data, see Mathias et al. 1997). It is noted from the middle panel of this figure that the second moment of  $\rho$  Puppis is dominated by the frequency  $2\omega$ , a situation that is typical in the case of an axisymmetric mode (see Aerts et al. 1992). The top panel of the figure shows that  $\langle v^3 \rangle$  is dominated by the frequency  $\omega$ . This is a general characteristic of the third moment since the term varying with  $\omega$  is influenced by all velocities together, i.e., by the rotation, the pulsation, and the intrinsic profile, while this is not the case for the other two terms (see Expression (12)).

The periodograms of the three moments can immediately be interpreted in terms of the periods that are present, while the corresponding phase diagrams of the moments are interpretable in terms of all the non-radial pulsation parameters. The basic idea is to compare the observed variations of the moments with theoretically calculated expressions for these variations for various pulsation modes, and so to determine the mode that best corresponds to the observations. This is achieved through the construction of a so-called discriminant, which is

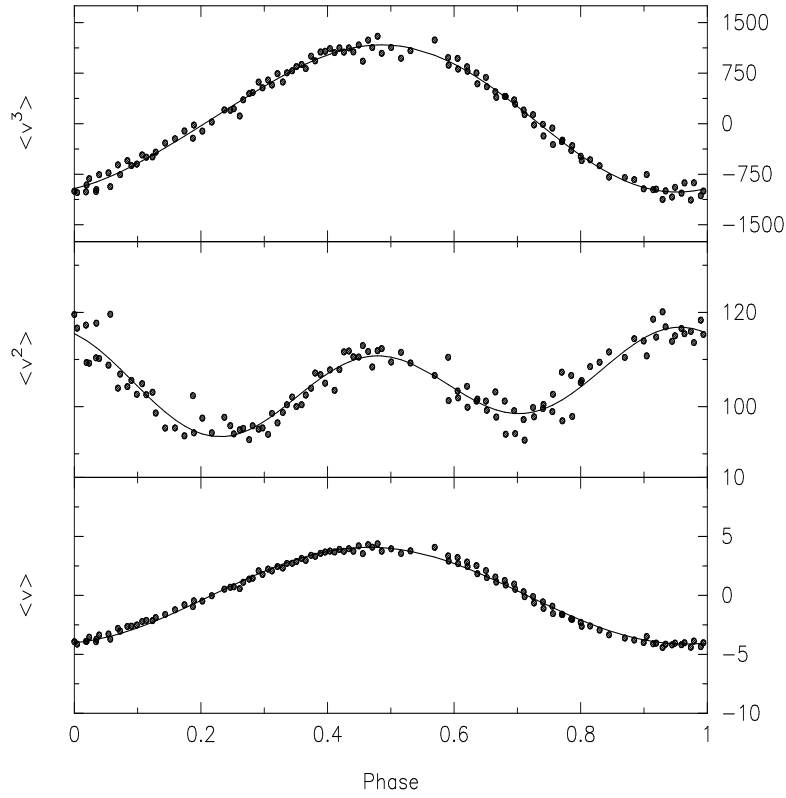


Figure 9. The three observed (dots) velocity moments of the Ca I  $\lambda\lambda 6122.21\text{\AA}$  line of  $\rho$  Puppis. The first, second, and third moments are expressed in respectively km/s,  $(\text{km/s})^2$ , and  $(\text{km/s})^3$ . The full line is a fit for a monopericodic pulsation model for the frequency  $f = 7.098168 \text{ c/d}$ . We refer to Mathias et al. (1997) for a complete description of the data.

based on the amplitudes of the moments:

$$\begin{aligned}
\Gamma_\ell^m(v_p, i, v_\Omega, \sigma) \equiv & \left[ \left| AA - v_p |A(\ell, m, i)| f_{AA} \right|^2 \right. \\
& + \left( \left| CC - v_p^2 |C(\ell, m, i)| \right|^{1/2} f_{CC} \right)^2 \\
& + \left( \left| DD - v_p v_\Omega |D(\ell, m, i)| \right|^{1/2} f_{DD} \right)^2 \\
& + \left( \left| EE - v_p^2 |E(\ell, m, i)| - \sigma^2 - b_2 v_\Omega^2 \right|^{1/2} f_{EE} \right)^2 \\
& + \left( \left| FF - v_p^3 |F(\ell, m, i)| \right|^{1/3} f_{FF} \right)^2 \\
& + \left( \left| GG - v_p^2 v_\Omega |G(\ell, m, i)| \right|^{1/3} f_{GG} \right)^2 \\
& + \left( \left| RST - v_p^3 |R(\ell, m, i)| - v_p v_\Omega^2 |S(\ell, m, i)| \right. \right. \\
& \left. \left. - v_p \sigma^2 |T(\ell, m, i)| \right|^{1/3} f_{RST} \right)^2 \left. \right]^{1/2}.
\end{aligned} \tag{13}$$

The functions  $f_{AA}, \dots, f_{RST}$  are weights given according to the quality of the fits to the moments. We refer to Aerts (1996) for their calculation and for a more detailed description and an evaluation of the discriminant.

To define a criterion for mode identification, we proceed as follows. The function  $\Gamma_\ell^m(v_p, i, v_\Omega, \sigma)$  is minimised for each set of values  $(\ell, m)$  :

$$\gamma_\ell^m \equiv \min_{v_p, i, v_\Omega, \sigma} \Gamma_\ell^m(v_p, i, v_\Omega, \sigma). \tag{14}$$

The “best solution” for  $\ell$  and  $m$  is defined as the one for which  $\gamma_\ell^m$  attains the lowest value; it then also provides values for  $v_p, i, v_\Omega$  and  $\sigma$ .

Our discriminant was thoroughly tested (Aerts 1996) and turned out to be more accurate compared to the one presented by Balona (1990), which is based on the first two moments only. As with line-profile fitting, both the wavenumbers  $(\ell, m)$  and all the other velocity parameters are derived. The moment method is particularly suited to identify lower-degree modes ( $\ell \leq 6$ ) in slow rotators. In this sense, it is completely complementary to the Doppler Imaging method. The reason for this limitation is that it uses integrated line profiles, because of which high-degree modes are almost completely canceled out in the moment variations. The code that calculates the minima of the discriminant as presented here is written in the statistical package GAUSS and is available upon request from the first author of this paper.

We recall that the discriminant is unable to find the sign of  $m$ , because the theoretical expressions for the moments have only been determined in the case that the Coriolis force can be neglected. A generalisation that includes the Coriolis force, and thus is able to derive the sign of  $m$ , has been done as well (Aerts, unpublished).

A generalisation of the moment method to multiperiodic pulsations has been proposed (Mathias et al. 1994a). From our study and the one by Aerts et al. (1994b) it is clear that the moment method is less accurate for multiperiodic stars, but still better than any other alternative in the case of slow rotation. The biggest problem in the treatment of multiperiodic variations is the appearance of long beat periods due to the interaction of the different modes. This effect requires many observations, well-spread over the total beat period. A second theoretical problem is that a discriminant constructed to identify all the present modes at the same time is numerically too involved to be of any practical use. We are thus obliged to identify each mode separately by means of the discriminant given in Expression (13). In this way, all the information present in the beat-terms is lost.

An application of the discriminant to the moments of  $\rho$  Puppis shown in Figure 9 is given in Table 2. Clearly, the main mode of  $\rho$  Puppis is a radial one

Table 2. The minima of the discriminant for the main mode ( $f = 7.098$  c/d) of  $\rho$  Pup

$\ell$	$ m $	$\gamma_\ell^m$	$v_p$	$i$	$v \sin i$	$\sigma$
0	0	0.08	5.6	—	15.3	6.5
1	1	0.13	10.0	$38^\circ$	14.8	5.9
2	1	0.17	12.1	$64^\circ$	16.4	2.2
1	0	0.18	5.0	$7^\circ$	19.6	1.7
2	2	0.23	15.0	$53^\circ$	10.3	4.8
$\vdots$	$\vdots$	$\vdots$	$\vdots$	$\vdots$	$\vdots$	$\vdots$

with a pulsation velocity amplitude of some 6 km/s. As already mentioned in Section 4.1, we found evidence of two additional frequencies in our data: 7.82 c/d & 6.31 c/d (Mathias et al. 1997). Their amplitudes are too low to achieve an unambiguous mode identification. They are not found in photometry so far.

Up to now, the moment method in the given formulation has mainly been applied to  $\beta$  Cephei stars (see e.g., Aerts et al. 1992, Mathias et al. 1994a,b, Aerts et al. 1994a,b) but also to two  $\delta$  Scuti stars (20 CVn: Mathias & Aerts 1996,  $\rho$  Puppis: Mathias et al. 1997). Previous attempts to identify modes in  $\delta$  Scuti stars with Balona's (1990) version of the moment method are presented by Mantegazza et al. (FG Vir: 1994) and by Mantegazza & Poretti (X Caeli: 1996). We have recently obtained a large data set of high-quality line-profile variations of 20 CVn to check our findings presented in the 1996 paper, which were based on only very few spectra. We will proceed with the reduction and analysis process of the new data sets in the forthcoming months (Mathias et al., in preparation).

THE major limitation of the moment method is the fact that no confidence intervals for the minima of the discriminant and the corresponding velocity parameters  $v_p, i, v_\Omega, \sigma$  are available. Therefore, the competing modes as listed in Table 2 are difficult to compare with each other. The standard error of the minimum and of the estimates for  $v_p, i, v_\Omega$  and  $\sigma$  is caused by observational noise, by

limitations of the model describing the line-profile variations due to non-radial pulsation, and also by numerical inaccuracies occurring in the determination of the moments, of the amplitudes of the moments, and of the minima of the discriminant. Unfortunately, no method is found up to now to determine these uncertainties. We are currently elaborating on a statistically founded method to try and estimate these standard errors. If we succeed in doing so, then the major drawback of this method will be overcome. Again, line-profile fitting for the best solutions found by the discriminant is helpful to check the result of the mode identification.

## 5. Comparison between the methods

We have already mentioned the main advantages and disadvantages for each of the three methods described above. We briefly review them in Table 3. The methods are complementary in the sense that one is suited for slow rotators with low-degree modes (moment method), another for rapid rotators with high-degree modes (Doppler Imaging) and the third (line-profile variation fitting) is very useful (moment method)/necessary (Doppler Imaging) as a check of the results obtained with the other two methods.

## 6. Conclusions and future developments

In this review, we have discussed the different mode-identification techniques that are currently used to study the non-radial pulsations in pulsating stars from observations of line-profile variations. Three basic methods are presented, are compared to each other and applications to real observations of  $\delta$  Scuti stars are described.

Line-profile variations offer a very detailed picture of the various aspects of the pulsation velocity field. On the other hand, photometric observations are easier to obtain on a long time-basis and are as such often superior for a very accurate determination of the pulsation frequencies, especially in the case

Table 3. The main properties of each of the three identification methods based on observed line-profile variations. LPF, DI, and MM stand for respectively line-profile fitting, Doppler Imaging, and the moment method.

	LPF	DI	MM
Deduced parameters	$\ell, m$ , ampl vsini, $\sigma, i$	$\ell, m?$	$\ell, m$ , ampl vsini, $\sigma, i$
Limitations	no	$v/v\text{sini} \leq 20\%$	$\ell \leq 6$
Multiperiodicity	no	easy	possible
Underlying physics	yes	no	yes
Standard errors	no	no	not yet
Computation time	long	short	in between
Additional modeling	no	necessary	as check

of lower-degree modes. High-degree modes hardly show up in photometry and can only be found from high-quality line-profile variation data. An example of additional modes being seen in spectra compared to photometry is presented by De Mey et al. (1998). They have analysed high-quality line profiles of the multiperiodic  $\delta$  Scuti primary of the double-lined spectroscopic binary  $\theta$  Tuc. The dominant frequency is the same in the photometric and spectroscopic data, but the second frequency that shows up in the spectra was never found before in photometry. This example confirms that the gathering of simultaneous photometry and spectroscopy is the best strategy to find a complete and accurate identification of all the appearing modes in multiperiodic stars.

Future possible improvements from a theoretical point of view concern on the one hand the development of mathematical expressions for the phase and amplitude in Fourier space in such a way that these quantities can be immediately interpreted in terms of the physical parameters of the pulsational velocity field. We also briefly mention that a new method of “Doppler Mapping” was recently presented by Berdyugina et al. (2000). They apply a spectral inversion technique to obtain maps of the surface corotating with the dominant pulsation mode. From these maps, they determine the pulsation degree and study the latitudinal distribution of the pulsation field. The method still needs to be further explored. Secondly, the inclusion of temperature variations during the pulsation cycle is still not accurately done, since an adiabatic pulsation is assumed while it is to be expected that non-adiabatic effects are important in the outer region of the atmosphere where the observed spectral lines are formed. Finally, the inclusion of centrifugal forces may be an improvement for the most rapid rotators. The latter is only necessary for stars rotating close to their break-up velocity.

From an observational point of view, large progress can be expected in the near future now that better and better detectors become available. For the short-period  $\delta$  Scuti stars, the major problem in obtaining high temporal and spatial resolution profiles is that the ratio of the integration time to the main pulsation period is rather high. This was one of the reasons why the application of the moment method to the stars FG Vir and X Caeli was not very successful. The abovementioned ratio in these cases was respectively 13% and 8%, while it amounts to only 1% for our profiles of  $\rho$  Puppis shown in Figure 4. For such high ratios, the pulsational motion is averaged out over a part of the cycle and this prevents unambiguous identifications, especially for multiperiodic stars.

An interesting new technique for the interpretation of line-profile variations is by working with cross-correlation functions instead of real spectra. Such a technique can be performed by means of current spectrographs such as ELODIE attached to the 1.93m telescope in the Haute-Provence Observatory. Our analysis of 20 CVn (Mathias & Aerts 1996) was already based on cross-correlation profiles and has shown that they perfectly contain the pulsational motion on the condition that the correlation is based on a suitable set of selected spectral lines. By using a cross-correlation function, one can significantly decrease the integration time and still obtain a high S/N ratio. At the same time, one can observe optically fainter stars with success. More accurate versions of ELODIE-type spectrographs are CORALIE, attached to the Swiss 1.2m telescope and FEROS, attached to the ESO 1.5m telescope, both situated at La Silla in Chile.



Finally, we would like to point out that mode identification from line-profile variations will become an important tool to obtain some information on the nature of the excited modes in stars belonging to the new class of  $\gamma$  Dor stars. For reviews on this new group of pulsating stars we refer to Krisciunas (1998) and to Zerbi (these proceedings). Since the multiperiodic variations detected in them have periods roughly a factor 20 longer than the period of the radial fundamental mode for such stars, high-order  $g$ -modes are believed to be the cause of the variability. However, there is yet no pulsation mechanism that can explain the onset and the maintenance of the pulsations in these stars.

Handler & Krisciunas have given subsequent updated lists of *bona fide* members of the group, which currently constitutes 13 members. We have recently taken the first steps towards the discovery of cool  $g$ -mode pulsators by searching for  $\gamma$  Dor stars in an unbiased sample of 39 new variable A2–F8 stars discovered by means of the Hipparcos mission (Aerts et al. 1999b). We have reported the discovery of 14 new  $\gamma$  Doradus variables among this unbiased sample. We primarily focussed on the limited group of new variables for which both Hipparcos and Geneva data are available, mainly because the latter allow an accurate determination of the effective temperature. It is very likely, however, that our more extended list of 200 unclassified variable A2–F8 stars of which no Geneva data are at our disposal contains more objects of this type. This seems to be confirmed by a recent analysis by Handler (1999).

In 1996, we also started a search for new  $\gamma$  Dor stars by means of ground-based Geneva photometry. Our search has resulted so far in the discovery of three new and some five suspected  $\gamma$  Dor stars (Eyer & Aerts, 2000). In order to firmly establish the  $\gamma$  Dor nature of all these new candidates we have started a long-term spectroscopic campaign with CORALIE in the course of 1997, which is still ongoing. We found line-profile variability from our high-resolution spectra for almost all candidates. Some of them, however, turn out to be binaries (Eyer & Aerts, in preparation).

Line-profile studies of  $\gamma$  Dor stars are still scarce. Examples in which a large amount of spectra have been obtained and analysed are given by Balona et al. (1996,  $\gamma$  Dor) and by Aerts & Krisciunas (1996, 9 Aur). The latter study is based on cross-correlations obtained with the (by now unmounted) spectrograph CORAVEL and showed convincingly that such correlation functions indeed contain a sufficient amount of information to characterise the pulsational behaviour.

It is clear that a combination of long-term photometry and spectroscopy is essential and the only way to study the multiperiodic variability in the  $\gamma$  Dor stars. The best observing strategy is the same as the one for the slowly pulsating B stars (Aerts et al. 1999a), which are also multiperiodic  $g$ -mode pulsators. At present, we do not yet have a sufficient amount of line profiles for our targets, but we will continue our monitoring of  $\gamma$  Dor stars with CORALIE during the forthcoming years. This will eventually lead to mode identifications, by applying the moment method.

## References

- Aerts, C. 1994, In *Pulsation, Rotation and Mass Loss in Early-Type Stars*, L.A. Balona, H.F. Henrichs, J.M. LeContel, Kluwer Academisch Publishers, 75
- Aerts, C. 1996, *A&A*, 314, 115
- Aerts, C., De Cat, P., Peeters, E., et al. 1999a, *A&A*, 343, 872
- Aerts, C., Eyer, L., Kestens, E. 1999b, *A&A*, 337, 790
- Aerts, C., De Pauw, M., Waelkens, C. 1992, *A&A*, 266, 294
- Aerts, C., Krisciunas, K. 1996, *MNRAS*, 278, 877
- Aerts, C., Mathias, P., Gillet, D., Waelkens, C. 1994a, *A&A*, 286, 109
- Aerts, C., Waelkens, C. 1993, *A&A*, 273, 135
- Aerts, C., Waelkens, C., De Pauw, M. 1994b, *A&A*, 286, 136
- Baade, D. 1984, *A&A*, 135, 101
- Baade, D. 1987, In *Physics of Be stars*, A. Slettebak, T.P. Snow, Cambridge University Press, 361
- Balona, L.A. 1986a, *MNRAS*, 219, 111
- Balona, L.A. 1986b, *MNRAS*, 220, 647
- Balona, L.A. 1987, *MNRAS*, 224, 41
- Balona, L.A. 1990, In *Progress of Seismology of the Sun and Stars*, Y. Osaki, H. Shibahashi, Lecture Notes in Physics, 367, 443
- Balona, L.A., Böhm, T., Foing, B.H., et al. 1996, *MNRAS*, 281, 1315
- Berdyugina, S.V., Korhonen, H., Schrijvers, C., Telting, J.H., 2000, In *The Be phenomenon in early-type stars*, M.A. Smith, H.F. Henrichs, ASP Conference Series, in press
- Buta, R.J., Smith, M.A. 1979, *ApJ*, 232, 213
- Campos, A.J., Smith, M.A. 1980a, *ApJ*, 238, 250
- Campos, A.J., Smith, M.A. 1980b, *ApJ*, 238, 667
- De Mey, K., Daems, K., Sterken, C. 1998, *A&A*, 336, 527
- De Pauw, M., Aerts, C., Waelkens, C. 1993, *A&A*, 280, 493
- Eyer, L., Aerts, C., 2000, submitted to *A&A*
- Gies, D. R., Kambe, E., Josephs, T. S., et al., 1999, *ApJ*, 525, 420
- Gies, D.R., Kullavanijaya, A. 1988, *ApJ*, 326, 813
- Handler, G., 1999, *MNRAS*, 309, 19
- Hao, J. 1998, *ApJ*, 500, 440
- Kambe, E., Osaki, Y. 1988, *PASJ*, 40, 313
- Kennelly, E.J., Brown, T.M., Foing, B.H., et al. 1998a, In *Precise Stellar Radial Velocities*, J.B. Hearnshaw, C.D. Scarfe, ASP Conference Series, 110, 53
- Kennelly, E.J., Brown, T.M., Kotak, R., et al. 1998b, *ApJ*, 495, 440
- Kennelly, E.J., Yang, S., Walker, G.A.H. 1992b, *PASP*, 104, 15
- Kennelly, E.J., Walker, G.A.H., Catala, C., et al. 1996, *A&A*, 313, 571
- Kennelly, E.J., Walker, G.A.H., Merryfield, W.J. 1992a, *ApJ*, 400, L71

- Krisciunas, K. 1998, In *New Eyes to See Inside the Sun and Stars*, F.L. Deubner, J. Christensen-Dalsgaard, D.W. Kurtz, Kluwer Academic Publishers, 339
- Lee, U., Saio, H. 1990, *ApJ*, 349, 570
- Lee, U., Jeffery, C.S., Saio, H. 1992, *MNRAS*, 254, 185
- Mantegazza, L., Poretti, E. 1996, *A&A*, 312, 855
- Mantegazza, L., Poretti, E., Bossi, M. 1994, *A&A*, 287, 95
- Mathias, P., Aerts, C. 1996, *A&A*, 312, 905
- Mathias, P., Aerts, C., De Pauw, M., Gillet, D., Waelkens, C. 1994a, *A&A*, 283, 813
- Mathias, P., Aerts, C., Gillet, D., Waelkens, C. 1994b, *A&A*, 289, 875
- Mathias, P., Gillet, D., Aerts, C., Breitfellner, M.G. 1997, *A&A*, 327, 1077
- Merryfield, W.J., Kennelly, E.J. 1993, In *New Perspectives on Stellar Pulsation and Pulsating Variable Stars*, J.M. Nemec, J.M. Matthews, Cambridge University Press, 148
- Osaki, Y. 1971, *PASJ*, 23, 485
- Schrijvers, C. 1999, PhD Thesis, University of Amsterdam, The Netherlands
- Schrijvers, C., Telting, J.H., Aerts, C., et al. 1997, *A&AS* 121, 343
- Smeyers, P. 1984, In *Theoretical problems in stellar oscillations*, Proc. 25<sup>th</sup> Liège International Astrophysical Colloquium, 68
- Smith, M. 1977, *ApJ*, 215, 574
- Smith, M. 1982, *ApJ*, 254, 242
- Smith, M. 1983, *ApJ*, 265, 338
- Smith, M.A., Fitch, W.S., Africano, J.L., et al. 1984, *ApJ*, 282, 226
- Telting, J.H., Schrijvers, C. 1997, *A&A*, 317, 723
- Townsend, R.H.D. 1997, *MNRAS*, 284, 839
- Unno, W., Osaki, Y., Ando, H., Saio, H., Shibahashi, H. 1989, *Nonradial oscillations of stars*, 2<sup>nd</sup> edition, University of Tokyo Press
- Vogt, S.S., Penrod, G.D. 1983, *ApJ*, 275, 661
- Vogt, S.S., Penrod, G.D., Hatzes, A.P. 1987, *ApJ*, 496, 127
- Wade, R.A., Rucinski, S.M. 1985, *A&AS*, 60, 471